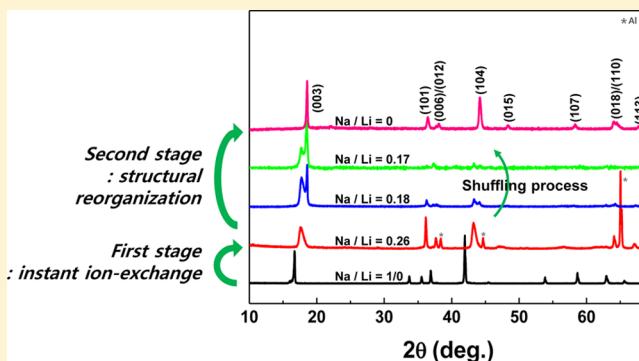


Ion-Exchange Mechanism of Layered Transition-Metal Oxides: Case Study of  $\text{LiNi}_{0.5}\text{Mn}_{0.5}\text{O}_2$ Hyeokjo Gwon,<sup>†,‡</sup> Sung-Wook Kim,<sup>§</sup> Young-Uk Park,<sup>†,⊥</sup> Jihyun Hong,<sup>†,⊥</sup> Gerbrand Ceder,<sup>||</sup> Seokwoo Jeon,<sup>\*,‡</sup> and Kisuk Kang<sup>\*,†,⊥</sup><sup>†</sup>Department of Materials Science and Engineering, Research Institute of Advanced Materials (RIAM), Seoul National University, 1 Gwanak-ro, Gwanak-gu, Seoul 151-742, Korea<sup>‡</sup>Department of Materials Science and Engineering, Korea Advanced Institute of Science and Technology (KAIST), 291 Daehak-ro, Yuseong-gu, Daejeon 305-701, Korea<sup>§</sup>Nuclear Fuel Cycle Process Development Group, Korea Atomic Energy Research Institute (KAERI), 989-111 Daedeok-daero, Yuseong-gu, Daejeon 305-353, Korea<sup>⊥</sup>Center for Nanoparticle Research, Institute for Basic Science (IBS), Seoul National University, 1 Gwanak-ro, Gwanak-gu, Seoul 151-742, Korea<sup>||</sup>Department of Materials Science and Engineering, Massachusetts Institute of Technology (MIT), 77 Massachusetts Avenue, Cambridge, Massachusetts 02139, United States

## S Supporting Information

**ABSTRACT:** An ion-exchange process can be an effective route to synthesize new quasi-equilibrium phases with a desired crystal structure. Important layered-type battery materials, such as  $\text{LiMnO}_2$  and  $\text{LiNi}_{0.5}\text{Mn}_{0.5}\text{O}_2$ , can be obtained through this method from a sodium-containing parent structure, and they often show electrochemical properties remarkably distinct from those of their solid-state synthesized equivalents. However, while ion exchange is generally believed to occur via a simple topotactic reaction, the detailed phase transformation mechanism during the process is not yet fully understood. For the case of layered  $\text{LiNi}_{0.5}\text{Mn}_{0.5}\text{O}_2$ , we show through ex situ X-ray diffraction (XRD) that the ion-exchange process consists of several sequential phase transformations. By a study of the intermediate phase, it is shown that the residual sodium ions in the final structure may greatly affect the electrochemical (de)lithiation mechanism.



## INTRODUCTION

Generally, an ion-exchange reaction refers to a class of chemical reactions between two materials that involve an exchange of one or more ionic components.<sup>1</sup> Certain inorganic crystal materials can react with ionic solutions to selectively remove one ionic component and replace it with other ions from the solution, with the end result being new materials. The ion-exchange process, based on topotactic reactions, can result in a material crystallographically analogous to the parent phase but with a new chemical composition. Thus, it is a simple and versatile method for exploring new compositions of materials having a certain crystal framework and is used widely in various fields.

In the field of lithium rechargeable batteries, this route of synthesis has been used frequently in designing new electrode materials for lithium storage.<sup>2–5</sup> Crystalline materials that are particularly suitable for alkaline ionic diffusion were considered as possible lithium-storing electrodes and were synthesized using this method. Armstrong et al. prepared, for the first time,

a layered  $\text{LiMnO}_2$ , analogous to a commercial  $\text{LiCoO}_2$ , from layered  $\text{NaMnO}_2$ . It had not been obtainable through conventional methods because of the relative instability of the layered structure over the orthorhombic phase.<sup>3</sup> The resulting layered  $\text{LiMnO}_2$  exhibits electrochemical properties fundamentally different from the orthorhombic  $\text{LiMnO}_2$ . More recently, Kang et al. succeeded in synthesizing a nearly perfect ordered layered  $\text{LiNi}_{0.5}\text{Mn}_{0.5}\text{O}_2$  in this way, taking advantage of the well-defined layered  $\text{NaNi}_{0.5}\text{Mn}_{0.5}\text{O}_2$ .<sup>2</sup> The ion-exchanged  $\text{LiNi}_{0.5}\text{Mn}_{0.5}\text{O}_2$  contrasted with  $\text{LiNi}_{0.5}\text{Mn}_{0.5}\text{O}_2$  from conventional solid-state synthesis routes in that the amount of lithium/nickel disorder was minimized in the structure.<sup>2,6–8</sup> The absence of blocking nickel ions in the lithium layer enabled significantly higher capacity delivery and boosted the power capability.<sup>2</sup>

While ion-exchange reactions have been used widely, often leading to the discovery of new materials, the details of the

Received: May 9, 2014

Published: July 17, 2014

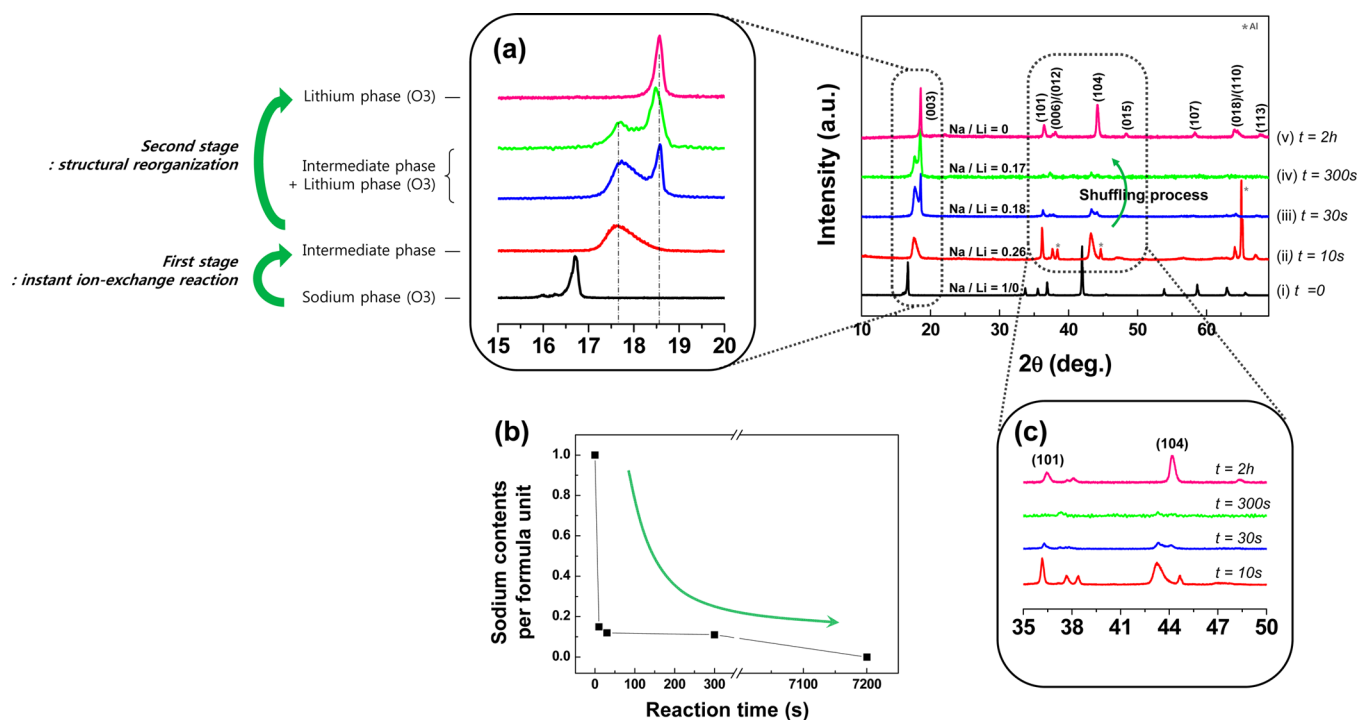


**Figure 1.** Ex situ XRD patterns of  $\text{Na}_x\text{Li}_{1-x}\text{Ni}_{0.5}\text{Mn}_{0.5}\text{O}_2$  during the eutectic molten salt ion-exchange process: (a) enlarged view around the main (003) peaks, (b) sodium contents per formula unit according to reaction time; (c) enlarged view around the (101) and (104) peaks, indicating the structural shuffling process.

mechanism and how the phase evolves during the reaction have yet to be revealed. In this case study of  $\text{LiNi}_{0.5}\text{Mn}_{0.5}\text{O}_2$ , we traced the structural evolution of the material by taking snapshots of the XRD patterns during the ion exchange. From the XRD patterns, we found that the ion-exchange process involved several sequential steps of phase transformations with notably different kinetics through an intermediate phase. In the study of the intermediate phase, we also discuss the role of the residual sodium content in the layered lithium phase.

## EXPERIMENTAL SECTION

$\text{NaNi}_{0.5}\text{Mn}_{0.5}\text{O}_2$  with an  $\alpha\text{-NaFeO}_2$  (space group  $R\bar{3}m$ ) structure was synthesized by a conventional solid-state reaction.<sup>2</sup>  $\text{Na}_2\text{CO}_3$  (Aldrich),  $\text{Ni}(\text{OH})_2$  (Aldrich), and  $\text{Mn}_2\text{O}_3$  (Aldrich) were used as precursors. In the ion-exchange process, the as-prepared  $\text{NaNi}_{0.5}\text{Mn}_{0.5}\text{O}_2$  powder (1 g) was mixed with a 10-fold excess amount of a eutectic composition of  $\text{LiNO}_3$  and  $\text{LiCl}$ . The mixture was heated at  $280^\circ\text{C}$  in air for various time periods. To control the ion-exchange kinetics and to obtain the intermediate phase, “softer” ion-exchange conditions were used, in which as-prepared  $\text{NaNi}_{0.5}\text{Mn}_{0.5}\text{O}_2$  samples (1 g) were added to a 10-fold lithium excess amount of a solution of 5 M  $\text{LiBr}$  (7.768 g) in hexanol (17.89 mL) at  $120^\circ\text{C}$  for 2 or 3 h.

For the electrochemical characterization, a slurry of 80 wt % active material, 10 wt % carbon black, and 10 wt % polyvinylidene fluoride (PVDF) dispersed in *N*-methyl-2-pyrrolidone (NMP) was prepared and cast on aluminum foil. The electrodes were dried at  $70^\circ\text{C}$  for 12 h. Electrochemical cells were assembled into a CR2016-type coin cell with a lithium metal counter electrode, a separator (Celgard 2400), and 1 M  $\text{LiPF}_6$  electrolyte in a 1/1 ethyl carbonate/dimethyl carbonate mixture in an Ar-filled glovebox. The charge/discharge tests were carried out between 2.5 and 4.6 V at a  $C/20$  rate using a potentiogalvanostat (WonA Tech, WBCS 3000) at room temperature.

Ex situ XRD measurements were carried out using a Rigaku D/MAX-RC diffractometer equipped with  $\text{Cu K}\alpha$  radiation by step scanning ( $0.01^\circ\text{ s}^{-1}$ ) in the  $2\theta$  range of  $10\text{--}70^\circ$ . The XRD measurement of the pristine  $\text{NaNi}_{0.5}\text{Mn}_{0.5}\text{O}_2$  for structural refinement was performed in an airtight holder to avoid moisture. On the other

hand, the ion-exchange process was monitored using a conventional holder, which resulted in a slight moisture contamination. Compositional analyses of the compounds were performed by inductively coupled plasma mass spectroscopy (ICP-MS, HP 4500).

## RESULTS AND DISCUSSION

Prior to the ion-exchange process, we synthesized the sodium precursor phase ( $\text{NaNi}_{0.5}\text{Mn}_{0.5}\text{O}_2$ ) with the  $\alpha\text{-NaFeO}_2$  structure (space group  $R\bar{3}m$ ) as a starting material.  $\text{NaNi}_{0.5}\text{Mn}_{0.5}\text{O}_2$  was found to be sensitive to moisture and susceptible to nickel oxide impurities; thus, all of the synthesis procedures had to be controlled carefully. Figure 1 presents the XRD pattern of the pristine  $\text{NaNi}_{0.5}\text{Mn}_{0.5}\text{O}_2$  at the bottom ( $t = 0$  s), confirming that the sodium phase was obtained successfully without impurities or second phases. All diffraction peaks correspond to those of  $\text{NaNi}_{0.5}\text{Mn}_{0.5}\text{O}_2$  with an O3 framework ( $a = 2.96\text{ \AA}$  and  $c = 15.90\text{ \AA}$ ; Figure S1, Supporting Information).<sup>2</sup>

The ion-exchange reaction for  $\text{NaNi}_{0.5}\text{Mn}_{0.5}\text{O}_2$  was carried out in a lithium-containing medium with intermittent pauses to probe the evolution of the phases by ex situ XRD. We adopted a eutectic molten salt method with  $\text{LiNO}_3$  and  $\text{LiCl}$  to reach the final stoichiometry,  $\text{LiNi}_{0.5}\text{Mn}_{0.5}\text{O}_2$ , from  $\text{NaNi}_{0.5}\text{Mn}_{0.5}\text{O}_2$ . The series of XRD patterns in Figure 1 from  $t = 0$  to 2 h illustrate the structural changes in the sample along with the reaction time and the corresponding Na/Li ratios. The characteristic change in the structure can be identified clearly by monitoring the (003) Bragg peak positions, as shown in Figure 1a.<sup>7,9,10</sup> We observed that two new peaks ( $17.7$  and  $18.6^\circ$ ) appeared almost immediately at the beginning of the reaction ( $10\text{ s} < t < 30\text{ s}$ ) with the disappearance of the (003) main peak of the pristine sodium phase. One of the two new peaks, that near  $18.6^\circ$ , corresponds to the characteristic (003) peak of  $\text{LiNi}_{0.5}\text{Mn}_{0.5}\text{O}_2$ . However, the broad peak near  $17.7^\circ$  could not be identified.

Nevertheless, these results suggest that the whole ion-exchange process can be divided into two major steps.

At the first stage of the ion exchange, which occurs within 10 s, a broad, unknown peak at  $\sim 17.7^\circ$  arises. This broad peak is located midway between the main peaks of the sodium and lithium layered phases, indicating that the intermediate phase is likely to be a layered structure with an intermediate slab space. During this stage, remarkably rapid sodium extraction and lithium insertion occurs. Sodium/lithium ratios from ICP results revealed that about 80% of the sodium/lithium exchange is complete within  $\sim 10$  s, as shown in Figure 1b. Considering that the particle size of  $\text{NaNi}_{0.5}\text{Mn}_{0.5}\text{O}_2$  is about  $1\ \mu\text{m}$  (Figure S2, Supporting Information), this fast exchange rate indicates high ionic diffusivity of both lithium and sodium in the material. We suggest that the rapid exchange reaction may cause sodium/lithium disordering in the lithium layers. The disordered nature of the sodium and lithium subsequently leads to a significant broadening of the (003) peak in the parent phase, as observed for the  $17.7^\circ$  peak at  $t = 10$  s. However, the second stage (from  $t = 10$  s to 2 h) resembled a two-phase reaction between the intermediate phase and the lithium phase. A sharp (003) peak of  $\text{O3-LiNi}_{0.5}\text{Mn}_{0.5}\text{O}_2$  at  $18.6^\circ$  arises as the ion exchange progresses, while the fraction of the intermediate phase decreases with the extended ion-exchange reaction. The conversion from the intermediate phase to  $\text{LiNi}_{0.5}\text{Mn}_{0.5}\text{O}_2$  is relatively slow and involves only a small change in the sodium content (Figure 1b). This indicates that a major structural evolution occurs at this stage with minimal exchange of sodium and lithium. During this stage, it is believed that the reorganization of the oxygen framework proceeds, toward a well-defined layered structure. The fact that the XRD evolution resembles a two-phase reaction indicates that the reorganization proceeds following a nucleation and growth mechanism of  $\text{O3-LiNi}_{0.5}\text{Mn}_{0.5}\text{O}_2$  at the expense of the intermediate phase. The second stage is accompanied by some structural “shuffling” process. Figure 1c shows that from  $t = 10$  to 300 s, almost all the XRD peaks decrease markedly in intensity versus the (003) main peak. This indicates that long-range ordering, within or among layers, was largely lost, while the layeredness was maintained. During this shuffling process, the structural reorganization, including the migration of sodium and lithium ions, is expected to randomize the stacking of  $\text{MO}_2$  ( $M =$  transition metal) slabs. Much complex rearrangement of oxygen layers can occur locally, such as sliding and dragging of oxygen layers or stacking faults, which may lead to the significant broadening of most Bragg peaks, except those for the (003) planes. After the shuffling process, the slabs are reordered into energetically stable stacking sequences, restoring the crystallinity. Figure 1c clearly indicates that peaks such as (104) and (101) are restored completely.

To understand the nature of the intermediate phase, which serves as an important medium in the ion-exchange process, we attempted to prepare a pure intermediate phase. However, it was difficult to achieve this through the given ion-exchange method, because the exchange kinetics was extremely fast. Instead, we used softer ion-exchange conditions based on hexanol at a lower temperature.<sup>11</sup> In this way, we obtained two intermediate-phase samples with slightly different Na/Li ratios: one with  $\text{Na/Li} \approx 0.29$  (IE1) and the other with  $\text{Na/Li} \approx 0.55$  (IE2). Figure 2 shows that the two samples shared similar XRD patterns and peak shapes, which are characteristic of the intermediate phase. However, the comparison of the (003) main peak positions of the two samples ( $\text{IE1} = 17.69^\circ$  and  $\text{IE2}$

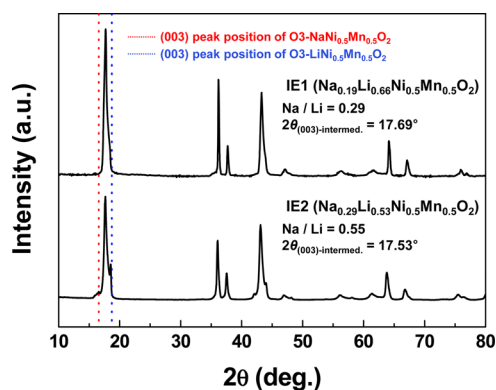


**Figure 2.** XRD patterns of intermediate phases (IE1 and IE2), fabricated by controlling exchange kinetics.

$= 17.53^\circ$ ) indicated that the slab spacing was larger in IE2 than IE1, consistent with the composition analysis showing that IE2 contained more sodium ions. The full pattern matching of the samples revealed that  $a = 2.90$  and  $2.91\ \text{\AA}$  and  $c = 15.04$  and  $15.15\ \text{\AA}$  for IE1 and IE2, respectively, but more detailed structural information could not be reliably extracted because of the width of the XRD peaks.

We investigated how the two intermediate phases would respond to (de)lithiation. This would be also informative in understanding the effect of its presence in the final  $\text{LiNi}_{0.5}\text{Mn}_{0.5}\text{O}_2$  on the electrochemical properties. Figure 3a,b shows the charge/discharge profile and the corresponding XRD patterns of the IE1 electrode. Interestingly, the main peak of the intermediate phase split into two peaks at the early stage of charging, indicating that two different layered frameworks arise: one with a larger slab space and the other with a smaller slab space. One of the peaks at  $18.30^\circ$  can be attributed to the (003) peak of  $\text{LiNi}_{0.5}\text{Mn}_{0.5}\text{O}_2$ , while the other corresponds to the characteristic slab space of the P-type sodium layered structure (shown schematically in Figure 3).<sup>12,13</sup> It is not yet clear whether the layered phase with the larger slab space is exactly a P-type sodium phase. However, the formation of a P-type layered phase is plausible in the presence of sodium ordering in the slab space, and the formation of delithiated  $\text{O3-Na}_x\text{Ni}_{0.5}\text{Mn}_{0.5}\text{O}_2$  is hardly expected due to its main peak position around  $16.58^\circ$ .<sup>14</sup> When the sodium content becomes relatively richer, during lithium extraction, local sodium reordering can occur, inducing the sliding of oxygen layers into a P-type structure. It is well known that sodium-deficient layered phases, such as  $\text{Na}_x\text{CoO}_2$ , are typically stable in a P-type structure and contain an enlarged slab space.<sup>15</sup> We suggest that the observed P-type sodium phase is likely to be P3, because O3 orderings can be converted to P3 without major bond breaking or re-formation of transition-metal–oxygen bonds.<sup>14,16</sup>

In addition to the formation of a P-type sodium phase, the segregation of sodium ions during the lithium deintercalation also results in locally lithium-rich regions. The appearance of the XRD peak at  $18.3^\circ$  supports the formation of  $\text{O3-LiNi}_{0.5}\text{Mn}_{0.5}\text{O}_2$  in the sample. Figure 3b shows that the O3 structure can be maintained with further delithiation, reminiscent of the typical electrochemical behavior of  $\text{LiNi}_{0.5}\text{Mn}_{0.5}\text{O}_2$ . For a clearer view of the structural evolution, Figure 3c plots the main peak positions of the intermediate phase, P-type layered sodium phase, and the O3 lithium phase with charge and discharge. It is clear that the slab space of the

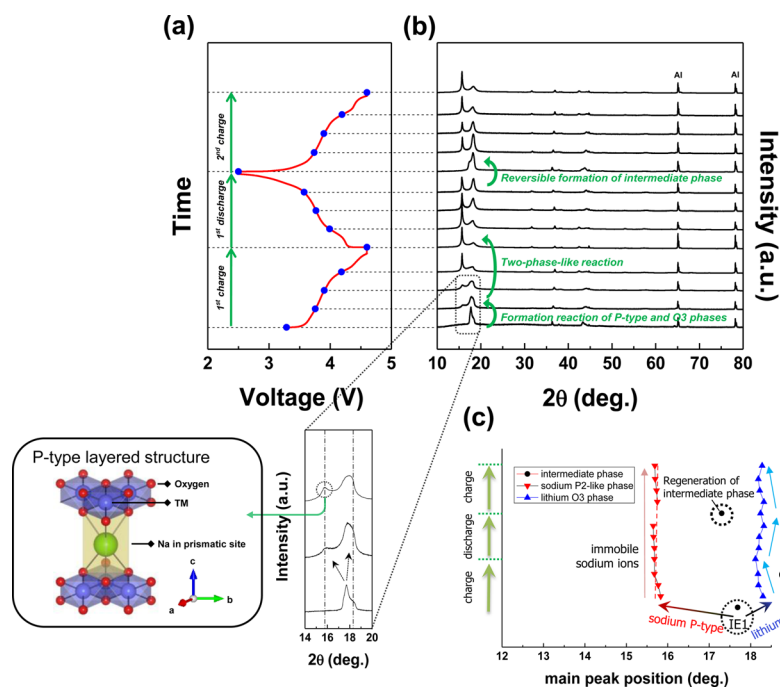


**Figure 3.** (a) Charge/discharge profile of IE1, (b) ex situ XRD patterns of IE1, enlarged view around the main peaks, and schematic view of a P-type layered structure, and (c) changes in the main peak positions of intermediate, sodium P-type, and lithium O3 phases during electrochemical (de)lithiation.

O3 lithium phase increases and decreases reversibly with extraction and insertion of lithium ions, confirming that the O3 phase is mainly a lithium-rich phase. However, the P-type layered phase hardly changed during charge and discharge, indicating that the sodium ions are not extracted electrochemically. Remarkably, the two-phase-like behavior between the P-type and O3 phases occurs simultaneously with the one-phase delithiation reaction of the O3 lithium phase. Moreover, the phase reaction is reversible, yielding the intermediate phase again when fully discharged to 2.5 V, although its intensity was lower than that of the initial state. The origin of this unusual behavior is not fully understood; however, the fact that the peak intensity of the intermediate phase decreases after a cycle indicates that the electrochemical annealing of the intermediate phase proceeds with cycling. Extended cycling eventually separated the O3 lithium phase and P-type sodium phase (Figure S3, Supporting Information). The electrochemical delithiation induces the segregation of sodium ions and the remaining lithium ions in the layer and subsequently leads to distinct orderings between layers.

To further understand the intermediate phase, similar experiments were carried out for IE2, with a slightly higher sodium content. Figure 4a,b presents the electrochemical profile and the corresponding XRD patterns. This material shows a tendency generally similar to that of the IE1 sample. However, unexpectedly, a new peak arose at a significantly lower angle, near  $12.7^\circ$ , on charging to around 4.2 V. The abnormally large  $d$ -spacing value does not correspond to any of the known layered transition-metal oxides. However, presumably, it involves the intercalation of solvent species that have a large molecule size into the layered structure. In the graphite anode, it is known that electrolyte intercalation, such as propylene carbonate, can occur,<sup>17</sup> while this phenomenon is hardly observed in cathodes.<sup>14,18</sup> We believe that the relatively large amounts of sodium ions in the mixed layered structure

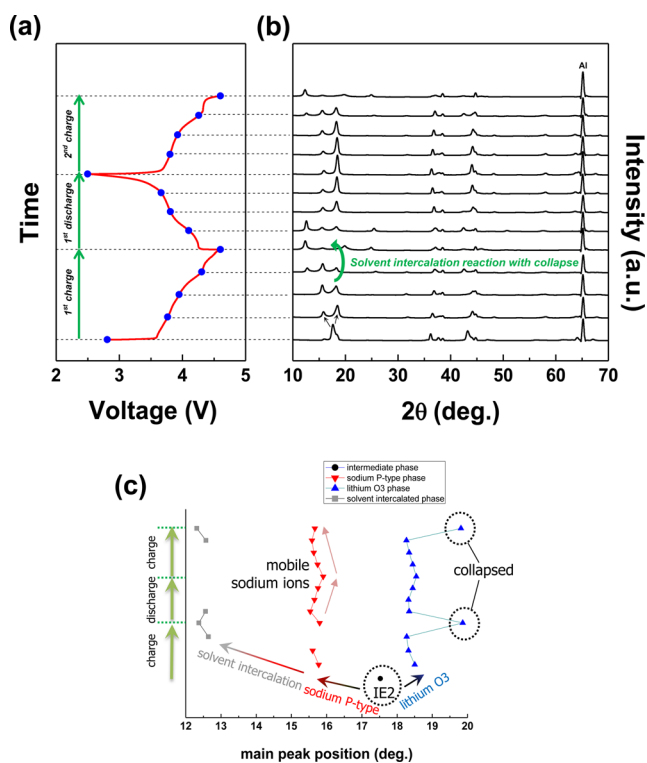


**Figure 4.** (a) Charge/discharge profile and (b) ex situ XRD patterns of IE2 and (c) changes in the main peak positions of intermediate, sodium P-type, and lithium O3 phases during electrochemical (de)lithiation.

could bring structural softness to the slab space, and the initially larger slab space of IE2 may have allowed the intercalation of solvent molecules into the structure. Another notable difference in IE2 is that the sodium ions in IE2 also partially participate in

the electrochemical reaction. Figure 4c shows that the main peak position of the P-type sodium phase shifted reversibly to lower and higher angles as the charge/discharge proceeded, in contrast to the behavior of the P-type phase in IE1. The participation of sodium ions in the electrochemical reaction was also confirmed by ICP tests for the charged sample of IE2 up to 4.6 V, showing a noticeable decrease in the sodium contents (from Na ~0.29 to ~0.21), which is consistent with the XRD results. We suggest that the generally larger slab space in the IE2 sample allowed reasonably fast sodium ion mobility in the structure, thus enabling the participation of sodium ions in the electrochemical reaction, in contrast to the immobile sodium ions in IE1. However, this active participation of sodium ion in IE2 results in the collapse of the slab space of the O3 lithium phase at the end of the charge. While the collapse of the layer space is generally observed for well-defined layered materials, such as lithium cobalt oxide at a highly charged state,<sup>19</sup> it indicates that the resulting O3 lithium phase is likely to be a well-defined layered structure; the absence of such a collapse in the IE1 sample indicates that the electrochemically less mobile sodium ions played the role of pillars, preventing the collapse. The full extraction of sodium in the IE2 sample could not prevent the collapse of the layer. The distinct behavior between IE2 and IE1 suggests that the sodium content in layered lithium oxides can affect the electrochemical behavior significantly and should be controlled carefully in the ion-exchange process.

## CONCLUSIONS

We investigated the ion-exchange mechanism by ex situ structural analyses of  $\text{NaNi}_{0.5}\text{Mn}_{0.5}\text{O}_2$  after different times of ion exchange. We found that ion exchange in this material was not a simple two-phase process but rather involved several intermediate complex compounds. In the early stage of ion exchange, the intermediate phase, which contains randomly distributed sodium and lithium ions in the lithium layers, forms almost immediately, with extremely fast exchange kinetics. Successively, a rather slower two-phase conversion occurred, involving a structural shuffling process. This ion-exchange process of  $\text{NaNi}_{0.5}\text{Mn}_{0.5}\text{O}_2$  exhibits behavior quite different from that in other literature reports that showed two-phase-like behavior without the formation of a stable intermediate phase.<sup>20,21</sup> This suggests that the ion-exchange mechanism varies with their composition and structure of the parent phase, which could affect the energetics of the sodium and lithium intermixed phase. We also investigated that the electrochemical delithiation behavior and structural evolution of the intermediate phases with different sodium contents indicates the importance of the residual sodium ions in the layered structure. The minor presence of sodium ions in the layers could prevent the collapse of the layer space, which is commonly observed in well-defined layered materials.

## ASSOCIATED CONTENT

### Supporting Information

Figures giving Rietveld refinement and an SEM image of pristine  $\text{NaNi}_{0.5}\text{Mn}_{0.5}\text{O}_2$  and the XRD pattern of the cycled intermediate phase. This material is available free of charge via the Internet at <http://pubs.acs.org>.

## AUTHOR INFORMATION

### Corresponding Authors

\*S.J.: e-mail, [jeon39@kaist.ac.kr](mailto:jeon39@kaist.ac.kr).

\*K.K.: e-mail, [matlgen1@snu.ac.kr](mailto:matlgen1@snu.ac.kr); tel, +82-2-880-7088; fax, +82-2-885-9671.

### Notes

The authors declare no competing financial interest.

## ACKNOWLEDGMENTS

This work was supported by (i) the Human Resources Development program (20124010203320) of the Korea Institute of Energy Technology Evaluation and Planning (KETEP) grant funded by the Korea government Ministry of Trade, Industry and Energy, (ii) the Energy Efficiency & Resources of the Korea Institute of Energy Technology Evaluation and Planning (Project no. 20112010100140) grant funded by the Korean government Ministry of Trade, Industry & Energy, and (iii) a grant from the Nuclear Research and Development Program of the National Research Foundation (NRF) funded by the Ministry of Science, ICT & Future Planning (MSIP), Republic of Korea.

## REFERENCES

- (1) Clearfield, A. *Chem. Rev.* **1988**, *88*, 125–148.
- (2) Kang, K.; Meng, Y. S.; Breger, J.; Grey, C. P.; Ceder, G. *Science* **2006**, *311*, 977–980.
- (3) Armstrong, A. R.; Bruce, P. G. *Nature* **1996**, *381*, 499–500.
- (4) Carlier, D.; Saadoune, I.; Croguennec, L.; Menetrier, M.; Suard, E.; Delmas, C. *Solid State Ionics* **2001**, *144*, 263–276.
- (5) Nazar, L. F.; Ellis, B. L.; Makahnouk, W. R. M.; Rowan-Weetaluktuk, W. N.; Ryan, D. H. *Chem. Mater.* **2010**, *22*, 1059–1070.
- (6) Schougaard, S. B.; Breger, J.; Jiang, M.; Grey, C. P.; Goodenough, J. B. *Adv. Mater.* **2006**, *18*, 905–909.
- (7) Breger, J.; Meng, Y. S.; Hinuma, Y.; Kumar, S.; Kang, K.; Shao-Horn, Y.; Ceder, G.; Grey, C. P. *Chem. Mater.* **2006**, *18*, 4768–4781.
- (8) Hinuma, Y.; Meng, Y. S.; Kang, K. S.; Ceder, G. *Chem. Mater.* **2007**, *19*, 1790–1800.
- (9) Johnson, C. S.; Kim, J. S.; Kropf, A. J.; Kahaian, A. J.; Vaughey, J. T.; Fransson, L. M. L.; Edstrom, K.; Thackeray, M. M. *Chem. Mater.* **2003**, *15*, 2313–2322.
- (10) Sathiy, M.; Hemalatha, K.; Ramesha, K.; Tarascon, J. M.; Prakash, A. S. *Chem. Mater.* **2012**, *24*, 1846–1853.
- (11) Paulsen, J. M.; Thomas, C. L.; Dahn, J. R. *J. Electrochem. Soc.* **1999**, *146*, 3560–3565.
- (12) Cabana, J.; Chernova, N. A.; Xiao, J.; Roppolo, M.; Aldi, K. A.; Whittingham, M. S.; Grey, C. P. *Inorg. Chem.* **2013**, *52*, 8540–8550.
- (13) Lu, Z. H.; Dahn, J. R. *J. Electrochem. Soc.* **2001**, *148*, A1225–A1229.
- (14) Komaba, S.; Yabuuchi, N.; Nakayama, T.; Ogata, A.; Ishikawa, T.; Nakai, I. *Inorg. Chem.* **2012**, *51*, 6211–6220.
- (15) Berthelot, R.; Carlier, D.; Delmas, C. *Nat. Mater.* **2011**, *10*, 74–80.
- (16) Delmas, C.; Braconnier, J. J.; Fouassier, C.; Hagenmuller, P. *Solid State Ionics* **1981**, *3–4*, 165–169.
- (17) Aurbach, D.; Eineli, Y. *J. Electrochem. Soc.* **1995**, *142*, 1746–1752.
- (18) Lu, Z. H.; Dahn, J. R. *Chem. Mater.* **2001**, *13*, 1252–1257.
- (19) Sun, D.; Kwon, C. W.; Baure, G.; Richman, E.; MacLean, J.; Dunn, B.; Tolbert, S. H. *Adv. Funct. Mater.* **2004**, *14*, 1197–1204.
- (20) Paulsen, J. M.; Larcher, D.; Dahn, J. R. *J. Electrochem. Soc.* **2000**, *147*, 2862–2867.
- (21) Tournadre, F.; Croguennec, L.; Saadoune, I.; Carlier, D.; Shao-Horn, Y.; Willmann, P.; Delmas, C. *J. Solid State Chem.* **2004**, *177*, 2790–2802.